Accepted Manuscript

A new approach for routine quantification of microplastics using Nile Red and automated software (MP-VAT)

Joana C. Prata, Vanessa Reis, João T.V. Matos, João P. da Costa, Armando C. Duarte, Teresa Rocha-Santos

Please cite this article as: J.C. Prata, V. Reis, J.T.V. Matos, et al., A new approach for routine quantification of microplastics using Nile Red and automated software (MP-VAT), Science of the Total Environment, https://doi.org/10.1016/j.scitotenv.2019.07.060

1 **A new approach for routine quantification of microplastics using Nile Red and automated**

2 **software (MP-VAT)**

3 Joana C. Prata[a*], Vanessa Reis[b], João T.V. Matos[c], João P. da Costa[d], Armando C. Duarte[e], Teresa

4 Rocha-Santos[f]

5

6

7 Centre for Environmental and Marine Studies (CESAM) & Department of Chemistry, University of
8 Aveiro, 3810-193 Aveiro, Portugal

9

10 **Corresponding author:**

11 Joana C. Prata, Centre for Environmental and Marine Studies (CESAM) & Department of Chemistry,
12 University of Aveiro, 3810-193 Aveiro, Portugal

13 Email: pratajc@ua.pt

14 Contact: +35191545801

15

16 a: pratajc@ua.pt

17 b: vanessa.reis@ua.pt

18 c: joaotvmatos@gmail.com

19 d: jpintocosta@ua.pt

20 e: aduarte@ua.pt

21 f: ter.alex@ua.pt

22 **A new approach for routine quantification of microplastics using Nile Red and automated**

23 **software (MP-VAT)**

24

25 **Abstract**

26 Microplastics are widespread contaminants in the environment. However, most identification

27 protocols rely on long and subjective visual counting, which could be improved using staining dyes.

28 Thus, the objective of this work is to identify the best staining dye protocol and create an objective

29 and quick automated counting software for microplastics. Tests were conducted to identify the

30 most appropriate of eight staining dye solutions and of six wavelengths for virgin and weathered

31 synthetic polymers, textile fibers, natural organic matter and filters. Nile Red produced the best

32 results (without interfering in infrared spectra) rendering microplastics fluorescent at 254 nm, but

33 with limited number of fluorescent polymers, and at 470 nm (with orange filter), with fluorescence

34 of plastics as well as natural organic matter (requiring a digestion step). Next, a script was

35 developed in ImageJ for the automatic quantification and characterization in shape (fiber,

36 fragment, particle) and size of fluorescent microplastics, the Microplastics Visual Analysis Tool

37 (MP-VAT). MP-VAT was evaluated, producing recovery rates in the range of 89.0 – 111.1% in

38 spiked filters under 470 nm. Furthermore, this package is accompanied by a script that sets a scale

39 from a known filter diameter, MP-SCALE, and a script that allows user threshold setting, MP-ACT.

40 **Keywords:** staining dyes; Nile Red; textile fibers; infrared spectra; small microplastics; nanoplastics

41

42 **1. Introduction**

43   Microplastics (plastics <5 mm) originate from intentional production (primary) or the

44   fragmentation of larger plastics (secondary), leading to widespread environmental contamination

45   (Ha and Yeo 2018). Monitoring concentrations of microplastics in the environment is essential to

46   better understand their sources and sinks. However, most microplastic quantification methods

47   rely on visual identification, highly amenable to operator biases and errors, thus exhibiting a high

48   degree of misidentification (Prata et al. 2019a). Nonetheless, this remains an important

49   inexpensive alternative to spectroscopic detection, and in most cases precedes this analysis.

50   Staining dyes, such as Nile Red (Erni-Cassola et al. 2017; Maes et al. 2017; Mason eta l. 2018; Shim

51   et al. 2016; Tamminga et al. 2017) or Rose Bengal (Kosuth et al. 2018; Liebezeit and Liebezeit

52   2014; Maes et al. 2017a; Ziajahromi et al. 2017), have been used to improve visual identification of

53   microplastics. By conferring color or fluorescence, microplastics can be easily differentiated from

54   mineral and organic materials in the sample. However, most staining protocols for microplastics

55   have been developed and used without any clarification regarding the ability to stain various virgin

56   and weathered polymers, and the lack of affinity for natural organic matter. Furthermore,

57   fluorescent microplastics can be photographed and automatically quantified by a counting

58   software, increasing sample throughput and removing the subjective variation inherent to

59   different operators. To the best of the authors' knowledge, this has only been attempted using

60   Galaxy Count (Mason et al. 2017), but results varied depending on the subjective selection of

61   threshold values. Thus, current staining dye protocols must be improved through a careful

62   evaluation of their affinity and selectivity for virgin and weathered polymers, as well as through

63   the use of detection software.

64   The objective of the present work was to select the most appropriate staining dye and wavelength

65   to selectively detect microplastics and to develop an automated counting script based on open-

66   source software that limits subjectivity in the quantification, resulting in a new approach for

67   quantification of microplastics in environmental samples. Therefore, virgin and weathered

68   polymers, as well as textile fibers and natural organic matter, were exposed to eight staining dye

69   solutions under two wavelengths (254, 365 nm), then selected the best staining dye (Nile Red) to

70   undergo selection of wavelengths (254 – 625 nm). Finally, these conditions were used to obtain

71   images to develop and validate the use of an automated counting software (Microplastics Visual

72   Analysis Tool) in ImageJ.

73

74   **2. Material and methods**

75   Procedures were conducted on synthetic and natural materials in order to explore the

76   identification of synthetic polymers by staining dyes and the confounding effect of other materials.

77   Staining dye solutions were chosen due to their previous use in microplastic samples (e.g. Nile

78   Red) or their affinity to stain lipophilic materials. Procedures took place to select the best of eight

79   staining dye solutions, followed by identification of the appropriate excitation wavelength for the

80   best solution. Determination of these conditions finally allowed the development of an automated

81   counting software (MP-VAT), which was properly evaluated and then used in environmental

82   samples.

83

84   **2.1. Staining dye solutions preparation**

85   Staining dye solutions tested were Acridine Orange (Riedel-de Häen, Germany), Basic Blue 24

86   (Sigma-Aldrich, U.S.A.), Crystal Violet (Merck, Germany), Lactophenol Blue (Labkem, Spain),

87   Neutral Red (Merck, Germany), Nile Red (Sigma Aldrich, U.S.A.), Safranin-T (Fluka, Germany),

88   Trypan Blue (Merck, Germany). Staining dye solutions of 0.01 mg ml^{-1} (Maes et al. 2017a) were

89   prepared in reagent grade ethanol (Fisher Scientific, U.K.) in amber glass bottles, except for Trypan

90   Blue which was dissolved in ultrapure water (owning to its low solubility in ethanol) and

91   Lactophenol Blue which was acquired as a solution and was diluted 50 times in ethanol.

92

93   **2.2. Sample collection for staining experiments**

94   Virgin polymers were obtained from Sigma-Aldrich (U.S.A.), namely low-density polyethylene

95   (LDPE), polypropylene (PP) and polystyrene (PS), or from consumer products with proper

96   identification, namely high-density polyethylene (HDPE), polyethylene terephthalate (PET),

97   expanded polystyrene (EPS), cellulose acetate (CA), polyvinyl chloride (PVC) and nylon. Weathered

98   polymers were collected in Barra beach, Aveiro, Portugal and identified by Fourier Transform

99   Infrared Spectroscopy (FTIR) as HDPE, polyethylene (PE), polyethylene fibers (PEf), PP, EPS and CA.

100   Based on the demand for fibers (Textile World 2015), the following textile fibers were store

101   bought or obtained from consumer products: cotton (100%), linen (100%), polyester (100%),

102   cotton and polyester (50% - 50%), polyamide (100%), viscose (100%), nylon (unknown), rayon

103   (unknown). Although nylon is considered a polyamide, nylon (from a stocking) was subsequently

104   considered separately from polyamide (fabric).

105   Organic materials were collected in Costa Nova beach, Aveiro, Portugal (*Fucus* genus algae,

106   driftwood, feathers, bivalve shell, charcoal) or store bought (fish muscle, shrimp chitin shell,

107   shrimp muscle, palm fat, paraffin). Filters of quartz (2.2 µm, Whatman QMA, U.S.A.), glass

108   microfiber (1.2 µm, Prat DUMAS, France), nitrocellulose (0.2 µm, GVS filter technology, U.K.),

109   mixed cellulose esters (0.45 µm, Gridded GN-6 White, GelmanSciences, U.S.A.), black

110   polycarbonate filters (PCTE, 0.2 µm, GE Healthcare Whatman, U.S.A.), C18 Octadecyl (12 µm, 3M™

111   Empore™, U.S.A.) were also subjected to staining to evaluate their possible interference in future

112   results.

113

114   **2.3. Staining dye solutions testing**

115   Following and adaptation of Ziajahromi et al. (2017) and Maes et al. (2017a), plastics, textile fibers

116   and natural organic matter were kept in glass flasks and subjected to 0.5 mL of staining dye

117   solution (enough to cover the sample), left to react for 30 minutes in the dark, washed with

118   distilled water in a mesh, and dried at 75ºC for 1 hour (Avangard.Line, BINDER, Germany), except

119   materials prone to melting, such as fat or paraffin, which dried over the counter overnight.

120   Afterwards, the samples were photographed (Canon IXUS 240HS) under visible light and two

121   wavelengths of UV-light (254 and 365 nm, VL-6.LC Vilber, Germany) to evaluate fluorescence.

122   Infrared spectrum of stained or fluorescent materials were obtained by Fourier transform infrared

123   spectroscopy attenuated total reflectance (FTIR-ATR) in a Perkin Elmer (U.S.A.) Spectrum BX FTIR

124   instrument at a resolution of 4 cm^{-1}, range of 4,000-600 nm and 32 scans.

125

126   **2.4. Wavelengths testing**

127   Nile Red was identified as the most efficient in coloring different types of polymers and synthetic

128   textiles under the first test conditions. In the literature, excitation wavelengths used for Nile Red

129   stained microplastics vary from 365 to 510 nm (Erni-Cassola et al. 2017; Maes et al. 2017a; Mason

130   et al. 2017; Shim et al. 2016; Tamminga et al. 2017), leading to differences in stained particles

131   emission and thus on microplastic quantification. To identify the optimal wavelength for the

132   excitation of Nile Red stained synthetic polymers, we tested under the same conditions the first

133   two wavelengths (254, 365 nm) and five more (395, 470, 495, 530, 625 nm) using forensic light

134   sources and filters FOCUS LED (SPEX Forensic, U.S.A.) on synthetic polymers, synthetic textiles,

135   natural organic matter and filters. Filters were orange for 470 and 495 nm (Standard ProMaster®

136   Orange Filter)., and red for 530 and 630 nm (Standard ProMaster® Red Filter).

137

138   **2.5. Development and evaluation of the image analysis software (MP-VAT, MP-ACT, MP-SCALE)**

139   Microplastic Visual Analysis Tool (MP-VAT) was developed in the freely available Image J

140   (https://imagej.nih.gov/), leveraging thresholding and analysis tools. Since users need to set a

141   scale for each picture, and most pictures will be filters with known diameters, a *macros* was also

142   developed to set a scale based on the diameter of a selection, MP-SCALE. Thus, filters with known

143   diameters can be used as scale by adjusting a circular selection over it (with "make ellipsoid" tool)

144   and running the aforementioned *macros*. Furthermore, a *macros* was developed that produces

145   similar results to MP-VAT, but allows the user to manually set the threshold, the Microplastics

146   Automated Counting Tool (MP-ACT). All scripts can be found in the Supporting Information (S.I.).

147   To understand the efficiency of microplastic detection by MP-VAT we have conducted a series of

148   evaluation procedures using: (a) images created on Adobe Photoshop CS6; (b) images created

149   digitally through a program developed in R named Microplastics R generated (MP-Rgen); (c)

150   photographs of spiked filters. In Adobe Photoshop CS6, a fluorescence particle was copied and

151   pasted in order to generate images ranging from 5 to 150 particles in intervals of 5. This rounded

152   particle was originally copied from a photograph of a polyethylene spiked sample in a glass fiber

153   filter stained with Nile Red (Canon 550D, EF-S 18-55 mm, F-stop F5.6, ISO 1600, exposure time

154   1/13 seg). The background of the images was generated by tiling and blurring (10) a background

155   area of the same photograph in order to mimic some of the noise. In R, a program was created

156   (MP-Rgen) in order to generate images with a known number of particles varying in size and

157   intensity. Ten images were generated by this method with particle numbers determined by the

158   random function in Excel, ranging from 1 to 50. Finally, a suspension of unknown concentrations of

159   very small shredded polyethylene (Sigma-Aldrich, U.S.A.) was prepared in ultrapure water and

160   filtered in varying volumes in glass fiber filters (in order to generate random numbers of particles),

161   stained with Nile Red, dried at 75ºC for 1 hour, and photographed (Canon 550D, EF-S 18-55 mm, F-

162   stop F5.6, ISO 1600, exposure time 1/13 seg). All images and photographs were quantified using

163   MP-VAT. Photographs of spiked filters were also quantified by two operators in order to compare

164   to MP-VAT results. Moreover, to test the general applicability of the method, 6L of tap water were

165   filtered in glass fiber filters and photographed using a different camera (Panasonic LUMIX FZ150)

166   by a different operator (**Figure S-7, S.I.**). Moreover, a 10 mL solution of 0.01 mg ml^{-1} of

167   polyethylene nanospheres (0.74 – 4.99 µm, 0.98 g cc^{-1}, Cospheric, U.S.A.) prepared in ultrapure

168   water were filtrated in a glass fiber filter and photographed under fluorescent microscopy (GFP

169   green fluorescent protein, Fluorescence Microscope Zeiss, Axio Imager 2 Zeiss, Germany).

170   Finally, MP-VAT was used in the quantification of fluorescent particles in real environmental

171   samples, namely water and sediment from a river in Aveiro, Portugal. Water was collected in glass

172   bottles (previously washed in acid, distilled water, and river water) capped with aluminum foil, and

173   500 ml filtered in glass fiber filters (GFFA, PratDUMA, France). In the case of sediments, these

174   were collected in a glass flask (previously washed in acid and distilled water), 200 ml of a solution

175   of 30% NaCl were added to 25 g of sediment (d.w) in a glass beaker, manually stirred with a glass

176   rod for 2 minutes, let to settle for 1 hour, and the supernatant filtered in glass fiber filters (GFFA,

177   PratDUMA, France)(adapted from Maes et al. 2017b). After drying, both filters were subjected to

178   organic matter removal through the application of a solution of 10 mL of 15% hydrogen peroxide

179   (H_2O_2) and 10 mL of 0.05 M of iron catalyst (Fe), left to react at 50ºC for 1h (Prata et al. 2019b),

180 washed with distilled water, dried, stained with Nile Red (0.01 mg ml^{-1}), washed with distilled

181 water, dried overnight at room temperature followed by 75ºC for 1 hour, and photographed under

182 470 nm using the orange filter (Canon 550D, EF-S 18-55 mm, F-stop F5.6, ISO 1600, exposure time

183 1/13 seg).

184

185 **3. Results & Discussion**

186 **3.1. Staining dye solutions evaluation**

187 **3.1.1. Virgin and weathered polymers**

188 Virgin and weathered polymers were subjected to 8 staining dye solution (0.01 mg ml^{-1}) exposed

189 to two wavelengths, 254 and 365 nm. Most polymers did not present significant coloration under

190 visible light, except for both virgin and weathered CA. Thus, under 0.01 mg ml^{-1}, the staining dye

191 solutions may not be suitable to aid visual identification without the use of a specific wavelength.

192 From the 8 staining dye solutions, Nile Red presented the best results as it made most synthetic

193 polymers fluorescent (**Table S-1 and S-2, S.I.**). Under 254 nm, LDPE, PET, PP, EPS and CA had

194 strong fluorescence, whereas HDPE, PS and PVC presented dim fluorescence (probably due to

195 their crystalline surface) and nylon presented no fluorescence. Worst results were obtained under

196 365 nm, where only LDPE, PP, EPS and CA presented fluorescence, but with lower intensities.

197 Spectrum of synthetic polymers did not suffer any significant change after staining with Nile Red

198 (**Figure S-1, S.I.**).

199 Other staining dye solutions did not present a good affinity for a large range of polymers.

200 However, some of these staining dye solutions may be useful for specific tests. For instance, under

201   254 nm, PET presented fluorescence with Acridine Orange (green) and virgin CA for Neutral Red

202   (yellow), Basic Blue 24 (purple), Acridine Orange (green) and Safranin-T (yellow).

203   Weathering, through changes in surface chemistry (Da Costa et al. 2018), may lead to changes in

204   the fluorescence of stained plastics. Fluorescence was observed in weathered HDPE, PP, EPS and

205   CA stained with Nile Red at 254 nm. However, weathered PE (both fragment and fiber) did not

206   present fluorescence under these conditions, even though virgin LDPE and HDPE did. Thus,

207   protocols using Nile Red under 254 nm light should be carefully implemented due to the potential

208   underestimation of PS, PVC, nylon and weathered PE in their samples.

209   Maes et al. (2017a) have proposed that the solvatochromic nature of Nile Red could lead to

210   different coloration of different types of polymers due to surface polarity. Thus, polar polymers

211   (e.g. nylon, PET) would present fluorescence in the red, whereas hydrophobic polymers (e.g. PE,

212   PP, PS) would present fluorescence in the yellow. This hypothesis is consistent with our results,

213   except for PS which presented orange fluorescence, and nylon, which was not fluorescent.

214   However, it is not possible to attest for this application in the case of weathered polymers, where

215   changes in polarity happen due to surface degradation, as only representatives of hydrophobic

216   polymers were tested. Thus, confirmation of this premise requires further research, which fell out

217   of the scope of the described work.

218

219   **3.1.2. Textile fibers**

220   Besides microplastics, synthetic fibers (i.e. microfibers) have a widespread use leading to their

221   presence in the environment (Dris et al. 2018). As with polymers, the 254 nm wavelength

222   produced the best results for textile fibers. Under this wavelength, for Nile Red stained textiles,

223   strong fluorescence was observed for linen, polyamide and rayon, whereas dim fluorescence was

10

224   observed for viscose, nylon, and polyester (**Table S-3, S.I.**). Thus, nylon may present different

225   fluorescence than polyamide due to differences in their chemistry or surface (e.g. thick crystalline

226   fiber in nylon, e.g. **Table S-3, S.I.**).

227   The low fluorescence of polyester under these conditions is almost imperceptible when the textile

228   is a mixture of polyester and cotton. Cotton and wool presented no fluorescence due to staining.

229   Wool presented red fluorescence in all treatments, but this is attributed to its original red color.

230   White-bluish fluorescence was also observed in white textiles, but not attributed to staining with

231   Nile Red. Even though fluorescence after Nile Red staining was observed for pieces of textile fibers

232   and fluffs (**Table S-6, S.I.**), the same was not observed for individualized fibers, a shortcoming of

233   this protocol.

234   Other staining dye solution may also be interesting in detecting some of these textiles. This is the

235   case of Acridine Orange and Safranin-T for linen and viscose, and Neutral Red, Basic Blue 24,

236   Acridine Orange and Safranin-T for rayon. Spectra of textile fibers did not suffer any remarkable

237   change after staining with Nile Red (**Figure S-2, S.I.**).

238

239   **3.1.3. Natural Organic matter**

240   Ideally, staining protocols should be able to stain synthetic polymers and textile fibers without

241   staining natural organic matter in the sample. If organic matter is stained, an extra step of removal

242   may be required. Thus, organic matter commonly found in beach sediments was tested.

243   No fluorescence was found for any of the staining dye solutions under both wavelengths (254 and

244   365 nm) for algae, driftwood, paraffin, feather, shrimp shell (chitin), bivalve shell (calcium

245   carbonate), charcoal and palm fat (**Table S-4, S.I.**). Only shrimp muscle and fish muscle presented

246   fluorescence when stained with Nile Red (both 254 and 365 nm) and with Safranin-T (365 nm).

247   However, muscle tissue is not likely to be abundant in microplastic samples since it is readily

248   consumed by organisms. Thus, staining dye solutions did not cause fluorescence in organic matter

249   under 254 and 365 nm light, except for muscle tissue.

250

251   **3.1.4. Filters**

252   Most microplastic sampling protocols involve a filtration step. Thus, it is expected that staining dye

253   solutions to be applied to filters containing microplastic samples. In order to correctly identify

254   microplastics, filters should not present fluorescence when stained. Thus, 6 types of filters were

255   subjected to the 8 staining dye solutions and two wavelengths.

256   Most filters presented visible coloration, but this was not always related to fluorescence under

257   UV-light. Nile Red presented fluorescence under 254 nm for all filters except for glass fiber and

258   PCTE (**Table S-5, S.I.**). Quartz, Nitrocellulose and Mixed Cellulose Ester filters also presented

259   fluorescence for Neutral Red, Acridine Orange and Safranin-T. Glass fibers presented fluorescence

260   for Acridine Orange and Safranin-T. Octadecyl filter was fluorescent in Neutral Red, Basic Blue,

261   Acridine Orange, Safranin-T. PCTE did not present fluorescence under any stain. Thus, glass fiber

262   and PCTE filters are recommended when using Nile Red staining dye protocols under 254 nm.

263

264   **3.2. Testing Nile Red sampled under multiple wavelengths (254, 365, 470, 495, 530, 625 nm)**

265   Nile Red was identified as the best of the 8 staining dye solutions tested under 254 and 365 nm.

266   Thus, virgin and weathered polymers, textiles, organic matter and filters stained with Nile Red

267   were exposed to wavelengths of 254, 365, 470, 495, 530 and 625 nm (**Table 1**). The objective was

268   to find the best wavelength to identify synthetic polymers.

269   [Table 1]

270   As observed herein, the 254 nm once again produced good results, leading to strong fluorescence

271   of most polymer types except for PS, PVC, nylon, virgin HDPE and weathered PE. Polyester, nylon,

272   rayon, linen and polyamide were also fluorescent. At this wavelength, organic matter does not

273   present fluorescence from staining (except for shrimp and fish muscle) whereas most filters are

274   fluorescent, with the exception of glass fiber and PCTE. At 365 nm, similar results to 254 nm are

275   obtained but with a lower fluorescence intensity, complicating detection. At 395 nm, no

276   fluorescence from Nile Red was observed.

277   At 470 nm, almost all polymers and all textiles (except nylon) showed strong fluorescence. Only

278   virgin HDPE and PVC and weathered PE fibers do no present fluorescence. At this wavelength,

279   quartz filters become less fluorescent (only in the edges), besides glass fiber and PCTE. However,

280   this wavelength leads to fluorescence of stained natural organic matter as well, namely, driftwood,

281   feather, shrimp and fish muscle and shrimp shell (chitin). Thus, the use of the 470 nm wavelength

282   requires a previous step of organic matter removal to ensure that the fluorescent particles are

283   indeed synthetic.

284   The 495 nm is also acceptable, with slightly less fluorescence, including of filters, which may be an

285   advantage. However, the fluorescence green background (of the countertop) and the dimmer

286   fluorescence of polymers may complicate identification. It is worth noting that Nile Red stained

287   weathered PE is only fluorescent under 470 and 495 nm (**Table S-7, S.I.**). At 530 nm, only CA and

288   most textiles (except for viscose and wool) are fluorescence. At 625 nm, no synthetic polymer,

289   textile fiber, natural organic material or filter is fluorescent.

290   Overall, the 254 and 470 nm were recognized as the best wavelengths to identify synthetic

291   materials. It is possible that commonly available lights in these wavelengths (and an orange filter

292   for 470 nm) are suitable for microplastic identification after Nile Red staining, allowing a cheap

293   identification method. The 470 nm has the advantage of revealing the fluorescence of PS, nylon,

294   weathered PE, and all the textiles (except nylon). The 254 nm has the advantage of a higher

295   contrast with the background (dark), no fluorescence of organic matter, but presents fluorescence

296   for only a limited number of synthetic materials. Furthermore, samples should always be dried

297   before being photographed, as wet samples generally presented lower fluorescent intensity when

298   compared to samples dried at 75ºC for 1 hour, a procedure that improves the identification of PVC

299   and PET under 470 nm (**Figure S-9**).

300

301   **3.3. Developing image analysis software in ImageJ**

302   **3.3.1. Development and use of MP-VAT**

303   Image J is a free software often used to analyze and automatically count particles, such as cells

304   (Forero et al. 2009; Grishagin 2015) and nanoparticles (Mahadevan et al. 2015; McQuaid et al.

305   2016). Thus, Image J could also be used to count fluorescent microplastics. Previous works have

306   used this software for manual counting of microplastics (Davidson 2012; Erni-Cassola et al. 2017;

307   Isobe et al. 2014; Isobe et al. 2017), but in none full automatization was attempted. Erni-Cassola et

308   al. (2017) stated to have written a *macros* for the detection of fluorescent microplastics, but there

309   was no evaluation and settings were situation specific, requiring subjective modification by each

310   user. Thus, the Microplastics Visual Analysis Tool (MP-VAT) was created to automatically count

311   fluorescent microplastics stained with Nile Red on ImageJ.

312 Using ImageJ functionalities, an automatic threshold was established capable of identifying

313 fluorescent particles, removing subjective selection of this parameter (**Figure 1**). Furthermore,

314 using circularity (varying from 0, for elongated shapes, to 1, for perfect circle), categories such as

315 fiber (0.0-0.3), fragments (0.3-0.6), and particles (0.6-1.0) were roughly defined (**Figure S-6, S.I.**).

316 Beside circularity (Circ) and area, the program also produces an approximation of the largest and

317 smallest dimension of the particle, presented respectively as Feret and MinFeret.

318 [Figure 1]

319 MP-VAT will be available in the tool bar as a button ("MP VAT") after installing

320 (Plugin>Macros>Install). Afterwards, the user must open an image (File>Open) and set a scale

321 manually (Analyze>Set Scale) or using the filter's diameter using MP-SCALE. With the area to be

322 analyzed selected (using the first or second button on the toolbar), the user only needs to click on

323 the "MP-VAT" button and wait for the process to finish. The results are automatically saved in the

324 same folder as the analyzed image as a .xls files, that can be opened in Microsoft Excel.

325 Filters with two backgrounds colors (e.g. clear edges and dark sample circle) may require setting

326 the scale using the filter and then selecting only the inner circle to be analyzed by MP-VAT.

327 Photography settings for each user may require testing before using MP-VAT in samples. For

328 instance, excess brightness may lead to faulty detection of particles (**Figure S-7, S.I.**). Limit of

329 detection will vary with the resolution and photography conditions (particles detected vary from 4

330 to 1 million pixels). Thus, it is of utmost importance that users always mention the scale used in

331 their MP-VAT analysis (Analyze>SetScale; e.g. 51 px mm^{-1}), since it will influence the lower limit of

332 detection for size (e.g. considering particles >3 px in a scale of 51 px mm^{-1} means MP-VAT will only

333 detect particles >0.05 mm). Large fragments may need to be removed from the sample through

15

334 sequential filtration as their strong fluorescence may compromise detection of smaller particles

335 and produce inconsistent results in MP-VAT due to the presence of a fluorescent halo.

336 MP-VAT has shortfalls regarding the lack of detection of color, polymer type and exact shape.

337 However, it overcomes some of the disadvantages of visual counting, such as objectivity, speed

338 and high throughput. Thus, MP-VAT constitutes a marked an improvement in the visual

339 quantification of microplastics. More information on MP-VAT can be found at

340 http://mpvat.wordpress.com.

341

342 **3.3.2. Evaluation of MP-VAT in the quantification of fluorescent particles**

343 MP-VAT evaluation was accomplished through three different techniques: (a) Adobe Photoshop

344 CS4 reconstruction of images with known number of particles (**Figure S-3, S.I.**); (b) digital

345 generation of a known number of particles using an R program (**Figure S-4, S.I.**); (c) polyethylene

346 spiked filters photographs (**Figure S-5, S.I.**). These three methods were chosen due to their

347 increasing complexity in image composition. Furthermore, due to their microscopic size,

348 polyethylene spikes were conducted in random concentrations followed by quantification by two

349 operators. Thus, the first two methods were used to assess the precision of quantification in

350 images where a nominal concentration is known.

351 In the first technique, MP-VAT was able to correctly quantify images generated in Adobe

352 Photoshop CS4 with a number of particles from 5 to 150, in intervals of 5, with an average

353 recovery rate of 100% (±0; **Table S-8, S.I.**). However, these particles offered little complexity. In

354 the second procedure, ten images containing a known number of blobs, between 0 and 50

355 (number randomly generated by Excel), were generated in R in MP-Rgen and processed in MP-

356 VAT, with a recovery range of 97.4 − 109.8%, with an average of 104.6% (**Table 2**). In this case,

357 overlapping particles were counted as a single particle, a limitation of MP-VAT that could also

358 occur in visual counting, or the digital separation of particles by watershedding created artificial

359 pieces from a single particle

360 [Table 2]

361 Five spiked PE samples were photographed under 470 nm (with orange filter) to calculate the

362 recovery of MP-VAT. As indicated in **Table 2**, the recovery rate for the quantification of fluorescent

363 particles is in the range of 96.9 – 105.3% between two different operators and of 89.0 – 111.1%

364 for MP-VAT (compared to the average count of the operators), with the average recovery for all

365 samples of 101.0% and 100.9% respectively, suggesting accuracy of both methods. In the

366 photographs analyzed, under our set conditions, the lowest size for the maximum particle

367 diameter (Feret) found was 65 µm for full filter photographs (~47 px mm^{-1}) and 0.65 µm for

368 fluorescence microscopy (~4.38 px µm^{-1}). The size of 0.65 µm found for PE nanospheres where

369 slightly smaller than that reported by the manufacturer (0.74 µm), possibly due to small errors

370 setting the scale or the presence of smaller particles.

371 The application of MP-VAT to real environmental samples, namely river sediment and water,

372 indicates its use even for complex matrices (**Figure 2**). In real environmental samples, chemical

373 digestion may be required to remove organic matter, fluorescent under 470 nm when stained with

374 Nile Red. The digestion protocol used (Prata et al. 2019b) wrinkled the filter, which did not

375 compromise the use of MP-VAT. Nonetheless, a digestion protocol must be developed in order to

376 preserve the filter structure while removing organic matter that may have fluorescent under 470

377 nm, and its success evaluated through micro-spectroscopy techniques.

378

379 **3.3.3. Using MP-ACT in samples contaminated with fibers or natural organic matter**

380   ImageJ can also be leveraged in cases of more conservative analysis using the 254 nm wavelength.

381   However, working in a clean room under a laminar-flow hood did not prevent filter contamination

382   with settling fibers, which have natural blue fluorescence under 254 nm, potentially leading to MP-

383   VAT estimation errors. The likely source of this contamination is the white cotton lab coat worn by

384   operators in this room. This could be justified by the use of fluorescent brightening agents in

385   textiles, which present fluorescence under UV light (Christie 1994). Thus, these fibers were not

386   fluorescent under 470 nm, in which no contamination was apparent and unlikely to happen after

387   the staining procedure.

388   As an alternative, we have quantified Nile Red fluorescent particles under 254 nm by selecting only

389   red particles using a color threshold. This was achieved by generating an image comprised only of

390   particles with a hue of 217 to 255, corresponding to violet to red (Saturation: 0-255; Brightness: 0-

391   255), and threshold color B&W (Image>Adjust>ColorThreshold), and counting them using MP-ACT,

392   which generated the same output table as MP-VAT but allows user threshold setting (**S-8, S.I.**).

393   Even though the use of MP-VAT is preferred, this method might offer an alternative to samples

394   rich in fiber cross-contamination or in non-removable natural organic matter. However, as

395   previously stated, not all microplastics are fluorescent under 254 nm (e.g. weathered PE) possibly

396   leading to an underestimation of microplastics in the sample. Furthermore, this method cannot be

397   subjected to evaluation or validation, as users are required to set threshold parameters.

398

399   **3.3.4. Next steps and future applications of MP-VAT**

400   Even though MP-VAT presented satisfactory results, more tests should be performed in order to

401   fully validate this method. In the future, MP-VAT should be validated using spikes of different

402   polymer types, compared to several independent counts by operators or techniques. The use of

403   MP-VAT on environmental samples should also be explored in more detail through coupling with

404   spectroscopic methods (e.g. micro-FTIR). Furthermore, the appropriate removal of organic matter

405   from samples prior to staining with Nile Red needs to be optimized in order for MP-VAT to

406   produce reliable results. This improvement, along with the optimization of sampling procedures,

407   could be used in harmony with MP-VAT, culminating into a single protocol of microplastic

408   identification that could be validated. Moreover, MP-VAT is not able to determine the chemical

409   composition of samples (i.e. polymer type) but allows simple and quick quantification and rough

410   characterization of size and shape of microplastic. Thus, it could be considered a complementary

411   procedure to spectroscopic methods. In the future, MP-VAT and spectroscopic methods (e.g.

412   micro-Raman) could be paired in order to produce a more complete characterization of

413   microplastic samples. This could be accomplished, for instance, by first running the spectroscopic

414   analysis, followed by staining and MP-VAT evaluation. Thus, MP-VAT presents a promising

415   complement for the routine quantification and characterization of microplastics.

416

4. Conclusion

418   A new approach for routine quantification of microplastics was developed using Nile Red coupled

419   with an automated counting software, MP-VAT. In a first test, eight staining dye solutions were

420   compared, leading to the selection of Nile Red as the most appropriate for the staining of

421   synthetic materials. A second test allowed the determination of the best excitation wavelengths

422   for synthetic materials stained with Nile Red, namely 254 and 470 nm. Finally, an automated

423   counting software (MP-VAT) was developed in ImageJ and evaluated, presenting promising results

424   for its application on microplastic samples. In the future, MP-VAT could be further tested and

425   improved by validation and comparison with reference techniques (e.g. spectroscopic methods).

426

427

Supporting Information

Supporting Information contains additional information about Fourier Transform Infrared

Spectroscopy (FTIR), photographs of stained materials, images used in the evaluation of MP-VAT

and all the scripts for the programs developed.

445

References

447   Christie R.M. (1994) Pigments, dyes and fluorescent brightening agents for plastics: An overview.

448   Polymer International 34, 351-361. http://doi.org/10.1002/pi.1994.210340401

449   Da Costa J.P., Nunes A.R., Santos P.S.M., Girão A.V., Duarte A.C., Rocha-Santos T. (2018)

450   Degradation of polyethyelene microplastics in seawater: Insights into the environmental

451   degradation of polymers. Journal of Environmental Science and Health, Part A, 53(9), 866-

452   875. https://doi.org/10.1080/10934529.2018.1455381

453   Davidson T.M. (2012) Boring crustaceans damage polystyrene floats under docks polluting marine

454   waters   with   microplastics.   Marine   Pollution   Bulletin   62,   1821-1828.

455   http://doi.org/10.1016/j.marpolbul.2012.06.005

456   Dris R., Gasperi J., Rocher V., Tassin B. (2018) Synthetic and non-synthetic anthropogenic fibers in

457   a river under the impact of Paris Megacity: Sampling methodological aspects and flux

458   estimations.   Science   of   the   Total   Environment   618,   157-164.

459   https://doi.org/10.1016/j.scitotenv.2017.11.009

460   Erni-Cassola G., Gibson M.I., Thompson R.C., Christie-Oleza J. (2017) Lost, but found with Nile red;

461   a novel method to detect and quantify small microplastics (20 um-1mm) in environmental

462   samples.   Environmental   Science   &   Technology   51(23),   13641-13648.

463   http://doi.org/10.1021/acs.est.7b04512

464   Forero M.G., Pennack J.A., Learte A.R., Hidalgo A. (2009) DeadEasy Caspase: Automatic Counting

465   of   Apoptotic   Cells   in   Drosophila.   PLoS   One   4(5):

466   e5441. https://doi.org/10.1371/journal.pone.0005441

467   Grishagin I.V. (2015) Automatic cell counting with ImageJ. Analytical Biochemistry 473, 63-65.

468   https://doi.org/10.1016/j.ab.2014.12.007

21

469   Ha J., Yeo M.-K. (2018) The environmental effects of microplastics on aquatic ecosystems.

470   Molecular & Cellular Toxicology 14(4), 353-359. https://doi.org/10.1007/s13273-018-

471   0039-8

472   Isobe A., Kubo K., Tamura Y., Kako S., Nakashima E., Fujii N. (2014) Selective transporto f

473   microplastics and mesoplastics by drifting in coastal waters. Marine Pollution Bulletin

474   89(1-2), 324-330. https://doi.org/10.1016/j.marpolbul.2014.09.041

475   Isobe A., Uchiyama-Matsumoto K., Uchida K., Tokai T. (2017) Microplastics in the Southern Ocean.

476   Marine   Pollution   Bulletin   114(1),   623-626.

477   https://doi.org/10.1016/j.marpolbul.2016.09.037

478   Kosuth M., Mason S.A., Wattenberg E.V. (2018) Anthropogenic contamination of tap water, beer,

479   and sea salt. PLoS ONE 13(4), e0194970. https://doi.org/10.1371/journal.pone.0194970

480   Liebezeit G., Liebezeit E. (2014) Synthetic particles as contaminants in German bears. Food

481   Additives   &   Contaminants: Part   A,   31(9),   1574-1547.

482   https://doi.org/10.1080/19440049.2014.945099

483   Maes T., Jessop R., Wellner N., Haupt K., Mayes A.G. (2017a) A rapid-screening approach to detect

484   and quantify microplastics based on fluorescent tagging with Nile Red. Scientific Reports.

485   7, 44501. http://doi.org/10.1038/srep44501

486   Maes T., Van der Meulen M., Devriese L.I., Leslie H.A., Huvet A., Frère L., Robbens J., Vethaak A.D.

487   (2017b) Microplastic baseline surveys at the water surface and in sediments of the North-

488   East   Atlantic.   Frontiers   in   Marine   Science   4,   136.

489   https://doi.org/10.3389/fmars.2017.00135

490   Mahedevan T.S., Milosevic M., Kojic M., Hussain F., Kojic N., Serda R., Ferrari M., Ziemys A. (2013)

491   Diffusion transport of nanoparticles at nanochannel boundaries. Journal of Nanoparticle

492   Research 15, 1477. https://doi.org/10.1007/s11051-013-1477-9

493   Mason S.A., Welch V.G., Neratko J. (2018) Synthetic Polymer Contamination in Bottled Water.

494   Frontiers in Chemistry 6, 407. http://doi.org/10.3389/fchem.2018.00407

495   McQuaid H.N., Muir M.F., Taggart L.E., McMahon S.J., Coulter J.A., Hyland W.B., Jain S.,

496   Butterworth K.T., Schettino G., Prise K.M., Hirst D.G., Botchway S.W., Currell F.J. (2016)

497   Imaging and radiation effects of gold nanoparticles in tumor cells. Scientific Reports 6,

498   19442. http://doi.org/10.1038/srep19442

499   Prata J.C., da Costa J.P., Duarte A.C., Rocha-Santos T. (2019a) Methods for sampling and detection

500   of microplastics in water and sediment: A critical review. Trends in Analytical Chemistry

501   110, 150-159. https://doi.org/10.1016/j.trac.2018.10.029

502   Prata J.C., da Costa J.P., Girão A.V., Lopes I., Duarte A.C., Rocha-Santos T. (2019b) Identifying a

503   quick and efficient method of removing organic matter without damaging microplastic

504   samples. Science of The Total Environment 686, 131-139.

505   https://doi.org/10.1016/j.scitotenv.2019.05.456

506   Shim W.J., Song Y.K., Hong S.H., Jang M. (2016) Identification and quantification of microplastics

507   using Nile Red staining. Marine Pollution Bulletin 113, 469-476.

508   http://dx.doi.org/10.1016/j.marpolbul.2016.10.049

509   Tamminga M., Hengstamann E., Fischer E.K. (2017) Nile Red Staining as a Subsidiary Method for

510   Microplastic Quantification: A Comparison of Three Solvents and Factors Influencing

511   Application Reliability. SDRP Journal of Earth Sciences & Environmental Studies 2(2).

512   http://doi.org/10.15436/JESES.2.2.1

513 Textile   World   (2015)   Man-Made   Fibers   Continue   To   Grow.   Retrieved   from:

514   https://www.textileworld.com/textile-world/fiber-world/2015/02/man-made-fibers-

515   continue-to-grow

516 Ziajahromi S., Neale P.A., Rintoul L., Leusch F.D.L. (2017) Wastewater treatment plants as a
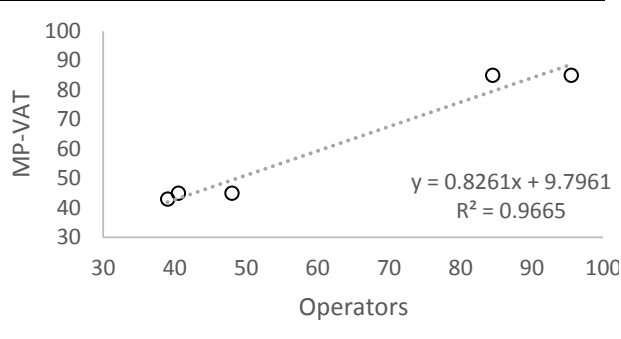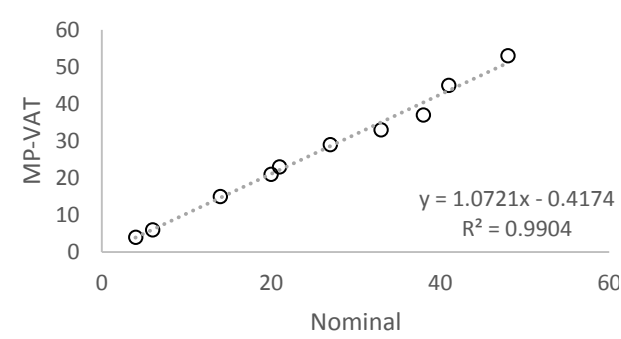
517   pathway for microplastics: Development of a new approach to sample wastewater-based

518   microplastics. Water Research 112, 93-99. https://doi.org/10.1016/j.watres.2017.01.042

519

520 **Table 2.** Recovery of fluorescent particles by MP-VAT compared to average operator count (in
521 spiked filters) and nominal number (in MP-Rgen).

Sample	Count		Recovery (%)		Pearson Correlation
Spiked filters	**Operators**	**MP-VAT**	**Operators**	**MP-VAT**	
	39	45	105.3	111.1	
	40.5	43	97.6	110.3	
	48	45	104.3	93.8	
	95.5	85	96.9	89.0	
	84.5	85	101.2	100.6	
	Mean (±S.D.)		101.0 (±3.8)	100.9 (±9.8)	
MP-Rgen	**Nominal**	**MP-VAT**	**MP-VAT**		
	4	4	100.0		
	6	6	100.0		
	14	15	107.1		
	20	21	105.0		
	21	23	109.5		
	27	29	107.4		
	33	33	100.0		
	38	37	97.4		
	41	45	109.8		
	48	53	110.4		
	Mean (±S.D.)		104.6 (±4.6)		

Spiked filters plot: $y = 0.8261x + 9.7961$, $R^2 = 0.9665$

MP-Rgen plot: $y = 1.0721x - 0.4174$, $R^2 = 0.9904$

25

522 **Tables & Figures**

523 **Table 1.** Fluorescence of virgin polymers, weathered polymers, textiles, natural organic matter, filters unstained and stained with Nile Red under
524 different wavelengths.

λ (nm)	Virgin Polymers Unstained	Virgin Polymers Nile Red	Weathered Polymers Unstained	Weathered Polymers Nile Red	Textiles Unstained	Textiles Nile Red	Natural Organic Matter Unstained	Natural Organic Matter Nile Red	Filters Unstained	Filters Nile Red
Vis										
254										
365										
395										
470										
495										
530										
625										

525 Virgin Polymers (left to right): low-density polyethylene (LDPE), high-density polyethylene (HDPE), polyethylene terephthalate (PET), polypropylene (PP), polyvinyl chloride (PVC), polystyrene (PS),
526 expanded polystyrene (EPS), cellulose acetate (CA), nylon. Weathered Polymers (left to right): PE, HDPE, PP, PE fibers, EPS, CA; PE-W: polyethylene. Textiles (left to right): cotton, cotton+polyester,
527 polyesters, viscose, nylon, wool, rayon, linen, polyamide. Natural Organic Matter (left to right): algae, driftwood, feathers, shrimp shell (chitin), shrimp muscle, fish muscle, shell (carbonate), carbon.
528 Filters (left to right): C18 octadecyl, black polycarbonate (PCTE), glass fiber, mixed cellulose esters, quartz, nitrocellulose.

529 **Figure 1.** Glass fiber filter spiked with PE, stained with Nile Red and photographed under 470 nm

530 (particles=53; 59.99 px mm^{-1}; A, B); glass fiber filters spiked with PE nanospheres and

531 photographed under fluorescent microscopy (particles=40; 4.40 px μm^{-1}; C, D).

532

533 **Figure 2.** Sample of 500 mL of river water filtered in a glass fiber filter (A), subjected to organic

534 matter removal, and photographed under 470 nm (particles=7; 49.42 px mm^{-1}; B, C); supernatant

535 of 25 g of river sediment separated by 30% NaCl and filtered in a glass fiber filter (D), subjected to

536 organic matter removal, and photographed under 470 nm (particles=32; 47.38 px mm^{-1}; E, F).

537

538   **Highlights**

539   • Nile Red was the best of eight dyes for staining microplastics
540   • Wavelengths of 254 and 470 nm produce the best results for Nile Red
541   • MP-VAT was developed for automatic quantification of fluorescent microplastics
542   • MP-VAT quantifies and characterizes microplastics based on shape and size
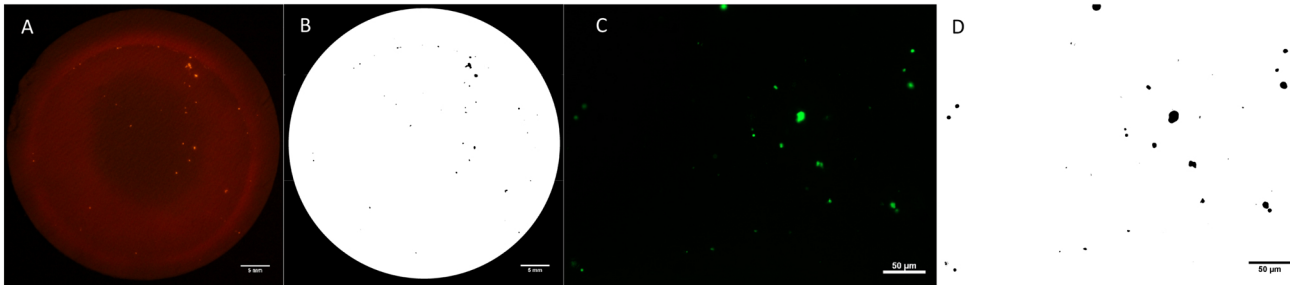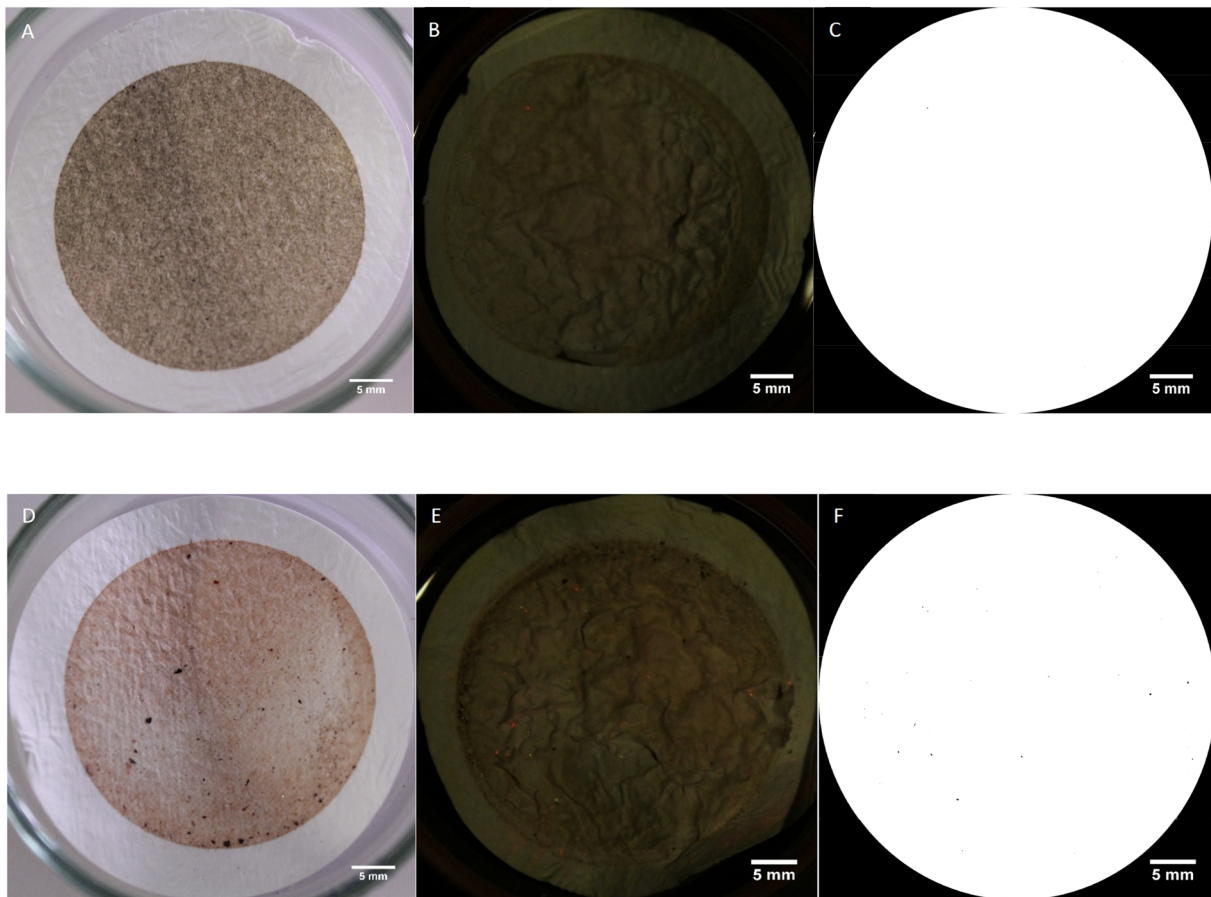543   • Recovery rates of 87.6–106.3% deem MP-VAT accurate for microplastic quantification

Figure 1

Figure 2